Evaluation of tissue-engineered human acellular vessels as a Blalock–Taussig–Thomas shunt in a juvenile primate model
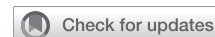
Kevin M. Nash, PhD,[a] Brian A. Boe, MD,[b] Sergio A. Carrillo, MD,[c] Andrew Harrison, AS, ARRT,[b] Ryuma Iwaki, MD,[d] John Kelly, MD,[b,d] Robert D. Kirkton, PhD,[a] Ramkumar Krishnamurthy, PhD,[e] Jeffrey H. Lawson, MD, PhD,[a,f] Yuichi Matsuzaki, MD, PhD,[d] Heather L. Prichard, PhD,[a] Kejal Shah, MD,[d] Toshiharu Shinoka, MD, PhD,[b,c,d] and Christopher K. Breuer, MD[d,g,h]

ABSTRACT

Objectives: Palliative treatment of cyanotic congenital heart disease (CCHD) uses systemic-to-pulmonary conduits, often a modified Blalock–Taussig–Thomas shunt (mBTTs). Expanded polytetrafluoroethylene (ePTFE) mBTTs have associated risks for thrombosis and infection. The Human Acellular Vessel (HAV) (Humacyte, Inc) is a decellularized tissue-engineered blood vessel currently in clinical trials in adults for vascular trauma, peripheral artery disease, and end-stage renal disease requiring hemodialysis. In addition to restoring blood flow, the engineered HAV demonstrates the capacity for host cellular remodeling into native-like vasculature. Here we report preclinical evaluation of a small-diameter (3.5 mm) HAV as a mBTTs in a non-human primate model.

Methods: We implanted 3.5 mm HAVs as right subclavian artery to pulmonary artery mBTTs in non-immunosuppressed juvenile rhesus macaques (n = 5). HAV patency, structure, and blood flow were assessed by postoperative imaging from 1 week to 6 months. Histology of HAVs and surrounding tissues was performed.

Results: Surgical procedures were well tolerated, with satisfactory anastomoses, showing feasibility of using the 3.5 mm HAV as a mBTTs. All macaques had some immunological reactivity to the human extracellular matrix, as expected in this xenogeneic model. HAV mBTTs remained patent for up to 6 months in animals, exhibiting mild immunoreactivity. Two macaques displaying more severe immunoreactivity to the human HAV material developed midgraft dilatation without bleeding or rupture. HAV repopulation by host cells expressing smooth muscle and endothelial markers was observed in all animals.

Conclusions: These findings may support use of 3.5 mm HAVs as mBTTs in CCHD and potentially other pediatric vascular indications. (JTCVS Open 2023;15:433-45)
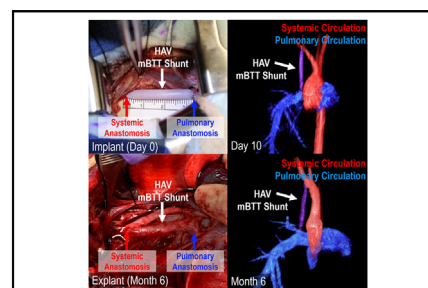
Implantation and angiography imaging of a 3.5 mm diameter HAV as a mBTTs in a NHP for 6 months.

CENTRAL MESSAGE

Preclinical evaluation of a 3.5 mm diameter Human Acellular Vessel (HAV) as a mBTTs in a non-human primate model demonstrated patency through 6 months and host cell repopulation of the engineered vessel.

PERSPECTIVE

Clinical use of ePTFE mBTTs as palliative treatment in CCHD has associated risks for thrombosis and infection. The 6 mm diameter HAV is in clinical trials for adult vascular indications and has demonstrated the capacity to repopulate with host cells. The successful implantation and evaluation of a 3.5 mm diameter HAV mBTTs in this nonhuman primate preclinical model suggests its potential for use in CCHD.

▶ Video clip is available online.

Cyanotic congenital heart disease (CCHD) results in decreased blood oxygenation, causing cyanosis in neonates. CCHD is associated with a high risk of developmental delay, arrhythmia, heart failure, cardiac arrest, and stroke. Several meta-analyses estimate a CCHD prevalence of ~1.5 per 1000 live births (5859 affected children per year in the United States).[1-3] Palliative surgical intervention is often required to alleviate symptoms of CCHD before proceeding to definitive repair of structural cardiac and vascular defects.

The first surgical treatment for CCHD was described by Drs Alfred Blalock and Helen Taussig[4] following pioneering preclinical work by Vivien Thomas.[5] The modified Blalock–Taussig–Thomas shunt (mBTTs) uses a synthetic vascular conduit, typically a 3 to 4 mm diameter expanded polytetrafluoroethylene (ePTFE) graft, anastomosed from the subclavian or innominate artery to the pulmonary artery as first described by Klinner and colleagues[6] and optimized by de Leval and colleagues.[7] This treatment redirects blood from the systemic to the pulmonary circulation, thereby increasing overall blood oxygenation. The mBTTs provides palliation in infants for 3 to 6 months, when they typically undergo definitive cardiac repair or staged single-ventricle palliation. Occlusion is the leading mBTTs failure mechanism and elevates risk of mortality, with up to 21% of shunts more than 50% occluded at time of elective takedown.[8] Shunt infection is also associated with longer hospital stays and greater in-hospital mortality in shunt recipients.[9]

The Human Acellular Vessel (HAV; Humacyte, Inc) is a decellularized tubular, tissue-engineered blood vessel consisting of human extracellular matrix proteins. The HAV is created by culturing human vascular cells within a biodegradable scaffold under carefully controlled biochemical and biomechanical conditions. The cultured vascular tissue is then decellularized to yield a mechanically robust and clinically nonimmunogenic conduit (Figure 1).[13] The 6 mm diameter HAV has been evaluated in eight phase 2 and phase 3 clinical trials, and has been implanted in more than 500 patients with more than 1000 patient-years of clinical exposure.

To generate smaller engineered blood vessels that may be suitable for pediatric cardiac surgery, the HAV-manufacturing platform was modified to produce small-diameter (3.5 mm) HAVs. The 3.5 mm vessels are 23 cm in length and have mechanical characteristics and composition comparable with the 6 mm vessels currently in clinical development. Since the HAV material has shown to be more resistant to infection than ePTFE,[14,15] the 3.5 mm HAV has potential as a mBTTs in CCHD. In this study, the 3.5 mm HAV was evaluated in a xenogeneic juvenile nonhuman primate (NHP) mBTTs model.

METHODS

3.5 mm HAV Production and Characterization

Small-diameter (3.5 mm) bioengineered HAVs were generated by modifying the previously described 6 mm × 42 cm HAV platform and production methods.[13,16] In summary, banked primary human vascular cells isolated from a single cadaveric donor were expanded and then seeded onto rapidly degradable polyglycolic acid tubular scaffolds having a 3.5 mm inner diameter. The seeded scaffolds were exposed to pulsatile cyclic distension within sterile bioreactors for 8 weeks of tissue culture. The cellular-engineered human vessel is then rendered acellular through a decellularization process as previously described.[17] HAVs were characterized before implantation by measuring suture retention strength, burst pressure, wall thickness, and collagen content.[18] Measurement of suture retention strength was performed in accordance with ISO 7198:2016 using an automated system.[19]

Animal Model and Surgical Implantation

A juvenile Old World primate model was chosen to (1) provide size and phylogenetic similarity to infant humans; and (2) attempt to minimize the potential for xenogeneic reactivity of the NHP to the human extracellular matrix of the HAV during long-term implantation.[13] All procedures were approved by the Institutional Animal Care and Use Committee of Nationwide Children's Hospital (protocol AR18-00149, March 7, 2019). Healthy male juvenile rhesus macaques (*Macaca mulatta*, n = 8, age 41-52 months) of Chinese origin were acquired from Orient BioResource. Three NHPs were used for development of the surgical model before evaluation of the HAV mBTTs in n = 5 NHPs. All nonhuman primates (NHPs) received humane care in compliance with the National Institutes of Health *Guide for the Care and Use of Laboratory Animals*. All operations and angiography procedures were performed in sterile fashion under general anesthesia.

Nonimmunosuppressed NHPs were implanted with a 3.5 mm HAV right-sided mBTTs between the right subclavian, carotid, or innominate systemic artery (SA, proximal) and pulmonary artery (PA, distal) via an open thoracotomy using standard surgical techniques. Heparin (100 U/kg) and phenylephrine were administered before clamping the target arteries. Proximal and distal anastomoses were created in an end-to-side manner with a running 7-0 PROLENE suture. Native blood flow through the PA was maintained (ie, pulmonary flow was supplied from both the PA and the mBTTs after completion of the operation). Radiopaque markers were sutured adjacent to the mBTTs anastomoses to mark HAV placement for in vivo imaging and postmortem evaluation. Acute patency of the implanted mBTTs was confirmed postoperatively by Doppler
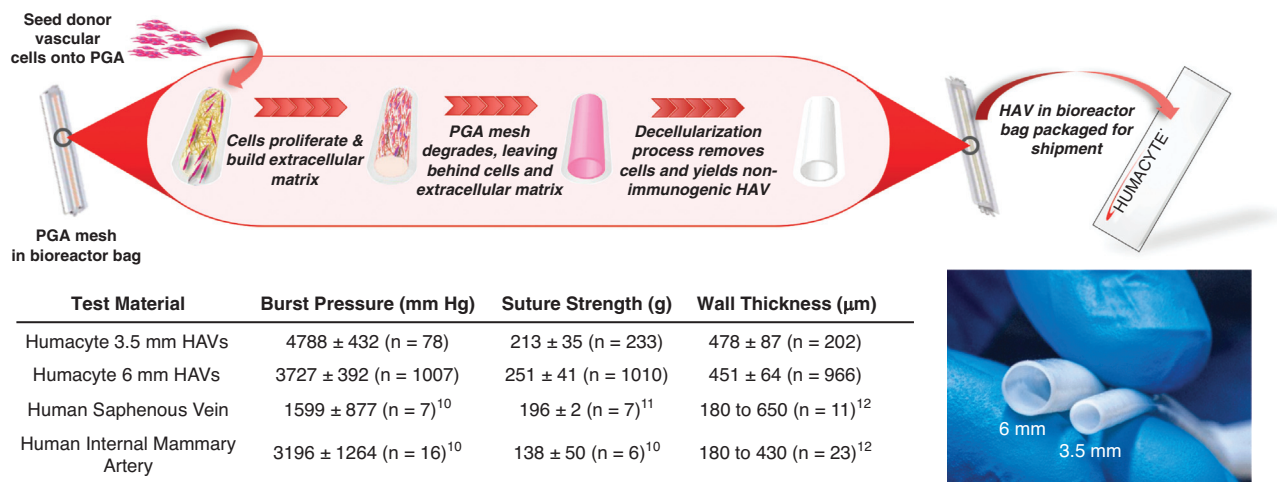
FIGURE 1. Development schematic and characteristics of 3.5 mm HAVs. HAVs are manufactured by seeding human vascular cells onto a polymer mesh scaffold within a bioreactor bag, culturing the cells to produce extracellular matrix as the polymer mesh degrades, and decellularizing the resulting tissue to remove cellular material. The resulting 3.5 mm and 6 mm inner diameter HAVs remain in a sterile bioreactor bag until opening in the operating room. Bioengineered HAVs have mechanical properties that are similar to human native blood vessels. Data for native human blood vessel characterization from Konig and colleagues,[10] L'Heureux and colleagues,[11] and Canham and colleagues.[12] *PGA*, Polyglycolic acid; *HAV*, Human Acellular Vessel.

echocardiography. Acute, intraoperative thrombosis of the HAV mBTTs in animal NHP2 occurred near the PA anastomosis. Patency was restored by placement of a bare metal stent (Integrity Coronary Stent, Medtronic; 9 mm length, expanded to 3.5 mm diameter) across this region, followed by completion of the procedure.

Pre- and postoperatively, NHPs were administered oral aspirin (3.5 mg/kg) daily throughout the study, and subcutaneous enoxaparin (10 mg) was administered for 30 days postoperatively. Throughout the study, NHPs were monitored by echocardiography and observed for clinical signs of congestive heart failure. Of the n = 8 total animals in this study, the initial n = 3 were used in the development of the surgical model and the subsequent n = 5 were survived for the planned 3- to 6-month evaluation.

Angiography

Fluoroscopic angiography of HAV mBTTs was performed 1 to 2 weeks postoperatively and before explant. The right femoral artery and femoral vein were accessed with separate angiographic catheters advanced to the aortic root and PA for systemic and pulmonary vascular imaging, respectively. HAV mBTTs and surrounding vasculature were visualized by iodinated contrast injections and captured by fluoroscopy (Infinix-i system; Canon Medical Systems, USA). Rotational angiography was performed with simultaneous systemic and pulmonary injections while the C-arm

rotated in a continuous movement around the region of interest. Measurements of graft and vessel diameters were performed using the Canon Infinix-i system. Three-dimensional reconstructions were generated using Vitrea software (Canon Medical Systems).

Magnetic Resonance Imaging (MRI)

MRI was performed at 1, 3, and 6 months as previously described.[20] MRI scans were captured on a Prisma 3T MRI (Siemens Medical Systems). Animals were sedated with continuous propofol infusion, intubated, and mechanically ventilated. Primates were administered ferumoxytol (5 mL/kg, intravenously) as a contrast agent. Black blood fast-spin echo MRI and contrast-enhanced 3-dimensional magnetic resonance angiography were obtained for anatomic imaging with HAV diameter measured at proximal, medial, and distal regions. Magnetic resonance 2-dimensional and 4-dimensional flow sequences were obtained to assess flow velocities and bulk flow through the graft (Video 1).

Histology

After the animals were humanely euthanized, a full necropsy was performed, and harvested tissues were fixed in 10% neutral buffered formalin. Representative sections of non-HAV tissues (heart, spleen, liver, kidney, brain, lung, lymph nodes, and thymus) were sent to StageBio for

TABLE 1. Outcomes of 3.5 mm HAV mBTT shunts in juvenile NHPs

Animal	Weight, kg	HAV mBTTs Length, cm	Implant duration, mo	Outcome
NHP1	6.0	2.5	3	Midgraft dilatation, HAV patent*
NHP2	5.1	4.0	4	Stented at implant, HAV patent
NHP3	5.3	3.0	6	Midgraft dilatation, HAV patent
NHP4	6.3	3.0	6	Planned takedown, HAV patent
NHP5	5.4	3.0	6	Planned takedown, HAV patent

HAV, Human Acellular Vessel; *mBTT*, modified Blalock–Taussig–Thomas shunt; *NHPs*, nonhuman primates. *Early termination.

histopathology evaluation following standard operating procedures. The HAV mBTTs were pressure-fixed, explanted en bloc, and then processed for paraffin embedding followed by histologic sectioning (5 μm thickness) and staining. Hematoxylin and eosin (H&E; StatLab reagents) and Picrosirius Red (ab150681; Abcam) staining were performed using standard techniques. Immunohistochemistry with fluorescence microscopy was performed as previously described.[21] Explanted tissue sections and tissue slides (American MasterTech) were immunostained for alpha-smooth muscle actin (α-SMA; Dako M0851), von Willebrand Factor (vWF; Abcam 179451), CD3 (Dako A0451), CD20 (Abcam ab9475), CD11b (Abcam 52478), and CD68 (R&D Systems MAB2040). Fluorescent secondary antibodies included anti-mouse IgG Alexa Fluor 488 (Thermo Fisher Scientific A-11001) and anti-rabbit IgG Alexa Fluor 594 (Thermo Fisher Scientific A-11012). Cell nuclei were counterstained with 4′,6-diamidino-2-phenylindole (Thermo Fisher Scientific EN62248). Brightfield H&E images were taken using an Olympus BX41 microscope with an Olympus DP25 camera and cellSens software. Polarized light (Picrosirius red) and fluorescence microscopy were performed using a Nikon TE2000U microscope with a Photometrics CoolSNAP HQ2 camera. Images were acquired and processed using μManager[22] and Fiji (ImageJ) software.[23]

RESULTS

Development and Characterization of 3.5 mm HAV

Generation of HAVs at different diameters and lengths has been previously reported.[13] The manufacturing platform (Figure 1) was minimally modified for the production of small-diameter tissue-engineered blood vessels, by reduction of silicone tube outer diameter and polyglycolic acid mesh inner diameter from 6 mm to 3.5 mm. Bioreactors were designed to allow culture of 3.5 mm HAVs that were 23- or 42-cm long. The 3.5 mm HAVs produced were comparable with 6 mm HAVs by suture retention and had similar burst pressure strength. Characteristics of both HAVs were similar to those of native vessels (Figure 1).[10-12] Decellularization was confirmed by staining with H&E to confirm the absence of visible nuclei, in addition to assays which verified minimal concentrations of residual β-actin protein, MHC I protein, and an absence of DNA bands greater than 200 bp by gel electrophoresis.[21]

Evaluation of 3.5 mm HAV in an NHP mBTTs Model

The 3.5 mm HAV mBTTs (2.5-4.0 cm in length) were implanted via a thoracotomy approach in healthy juvenile rhesus macaques (3-4 years, 5.1-6.3 kg) with the proximal anastomosis to the innominate, right subclavian, or right carotid artery; and the distal anastomosis to the right PA. Target PA and SA diameters in these juvenile rhesus macaques (3.4-6.2 mm and 2.3-3.0 mm) were similar to those of human infants (approximately 4.1 mm and 2.9 mm, respectively).[24]

Model development animals (n = 3) were used to optimize the complicated surgical implantation procedure and postoperative care, and were followed up to 10 days postoperatively. During the development of the model, the HAV-to-PA anastomosis was found to be challenging due to the thin wall of the juvenile macaque PA.[25] A longitudinal arteriotomy was initially used for the PA anastomosis, similar to that used when anastomosing more rigid ePTFE mBTTs,[24] but this caused flattening of the HAV distal anastomosis upon tightening of the sutures, leading to intraoperative thrombosis. Subsequent implantations optimized the HAV-to-PA anastomotic approach by creating a circular arteriotomy matching the diameter of the HAV.

Longitudinal Evaluation of HAV mBTTs

After completion of the 3 model development implantations, we undertook 5 additional HAV implantations into the experimental animals (Table 1). All animals remained healthy throughout the study and there were no adverse events attributed to the implanted HAV. Implanted HAV mBTTs were evaluated by angiography and MRI through 3 to 6 months, similar to the median duration of mBTTs palliation in infants with CCHD.[26] All HAV mBTTs were patent by angiography 1 to 2 weeks post-implant, and at all time points before termination (Figure 2). Midgraft dilatations were noted in 2 of the 5 experimental animals: NHP1 at 3 months and NHP3 at 6 months post-implant. The corresponding regions in these grafts were further investigated by histology, as discussed later.

By noninvasive MRI flow imaging (Figure 3), blood flow through the mBTTs systemic-to-pulmonary circuit was 911 ± 167 mL/min (n = 3) and 473 ± 205 mL/min (n = 5) at 1 and 3 months, respectively (Figure 3, A and E). Blood flow through mBTTs in human infants ranges from 256 to 2400 mL·min^{-1}·m^{-2} (81.9-768 mL/min for 5.5 kg [0.32 m^2 body surface area]), making these flow rates comparable with those observed clinically.[27] The ascending aortic blood flow rate in the juvenile rhesus was approximately 1430 mL/min (n = 1). Luminal diameters of mBTTs at the proximal, midgraft, and distal regions (Figure 3, B-D) measured by MRI correlated well with measurements by fluoroscopy at termination (additional data in Figure E1). Some stenosis (luminal diameter: 2.28 ± 0.63 mm) was observed within all HAV mBTTs through 3 months (n = 5/5), and moderate stenosis (1.40 ± 0.42 mm) was observed in 2 of the 3 mBTTs evaluated at month 6. Narrowing in all mBTTs predominantly occurred near the PA anastomosis (Figure 3, F).

Explant Histology

HAV mBTTs were explanted at month 3 (NHP1), month 4 (NHP2), and month 6 (NHP3-5) and evaluated by histology. Sections stained with H&E showed remodeling of the 3.5 mm diameter HAV with host cells similar to that observed in previous preclinical and clinical studies of the 6 mm diameter HAV.[13,21] Infiltration of host cells was observed as early as 10 days post-implantation (Figure 4, A; model development NHP) and progressed to near-complete recellularization of the HAV wall, as well as creation of surrounding neoadventitial tissue, in the 3, 4, and 6
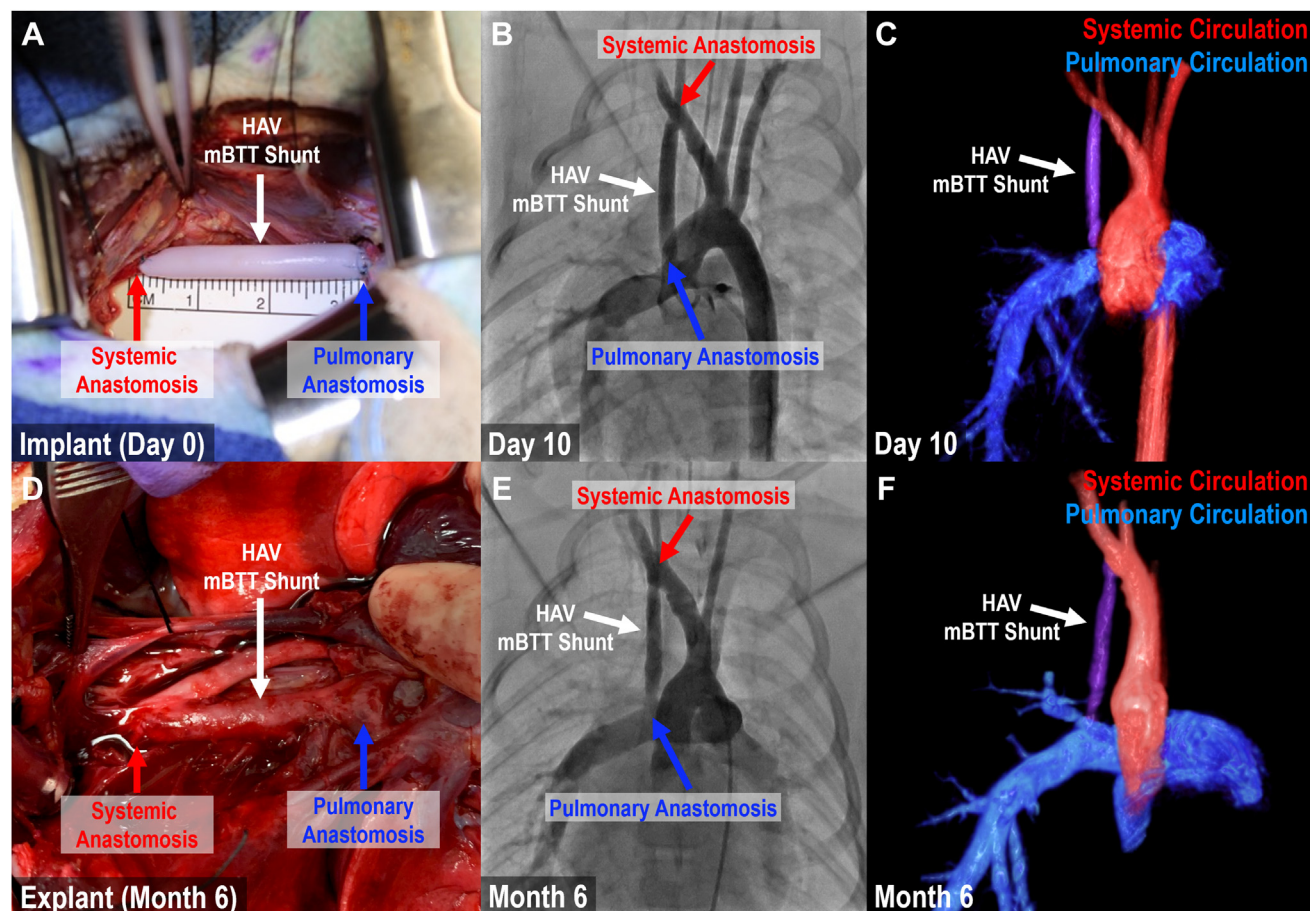
FIGURE 2. Surgical implantation and evaluation of 3.5 mm HAV mBTT shunts in juvenile rhesus macaques for 3 to 6 months. Representative photographs of a 3.5 mm HAV mBTT shunt at implant (A) and at 6 months (D) in NHP4. The HAV mBTT shunt was evaluated at 1 to 2 weeks (B and C) and 6 months (E and F) by fluoroscopy and 3-dimensional rotational angiography, respectively. The HAV mBTT shunt in NHP4 remained patent for 6 months and was found to be well incorporated into the host tissue at explant. *HAV*, Human Acellular Vessel; *mBTT*, modified Blalock–Taussig–Thomas shunt; *NHP*, nonhuman primate.

month explant samples (Figure 4, *B-D*). In addition, stent placement at implant within the mBTTs in NHP2 did not adversely impact host cell infiltration or remodeling of the HAV (Figure E2). Pannus ingrowth was noted in the distal regions of all grafts near the PA anastomosis, which correlated with graft stenosis.

Immunostaining revealed that most cells repopulating the wall of HAVs expressed α-SMA, a vascular smooth muscle marker (Figure 4, *E-H*). Additionally, many cells lining the HAV lumen expressed vWF, an endothelial cell marker, as early as 3 months post-implantation (Figure 4, *I-L*), suggesting the formation of luminal endothelium. Picrosirius red–stained tissue sections visualized under polarized light showed dense collagen I (orange–red) fibers with some collagen III (green–yellow) fibers[28] throughout HAV mBTTs explants at all time points (Figure 4, *M-P*). Average wall thickness measurements of explanted HAVs by histology (964 ± 360 μm) are similar to the initial 3.5 mm HAV

wall thickness (729 ± 144 μm) and did not appear to trend with implant duration.

HAV mBTTs explanted from these nonimmunosuppressed rhesus macaques revealed varying levels of immune cell infiltration, as demonstrated by small clusters of T cells (CD3$^+$) and B cells (CD20$^+$) surrounding grafts from NHP2, NHP4, and NHP5 (Figure 5, *A-I*). In NHP1 and NHP3, there were substantial populations of T and B cells, monocytes (CD11b$^+$), and macrophages (CD68$^+$) that had infiltrated the walls of the 2 HAV mBTTs. These were the 2 animals that developed dilatation of the implants over time (Figure 5, *J-O*). The most concentrated areas of immune and inflammatory cells were found within the midgraft dilatations, suggesting a correlation between host immune reactivity and dilatation of the HAV.

This type of adaptive immune response to an implanted HAV, accompanied by dilatation, has not been observed in baboons, nor in any human explant samples analyzed to
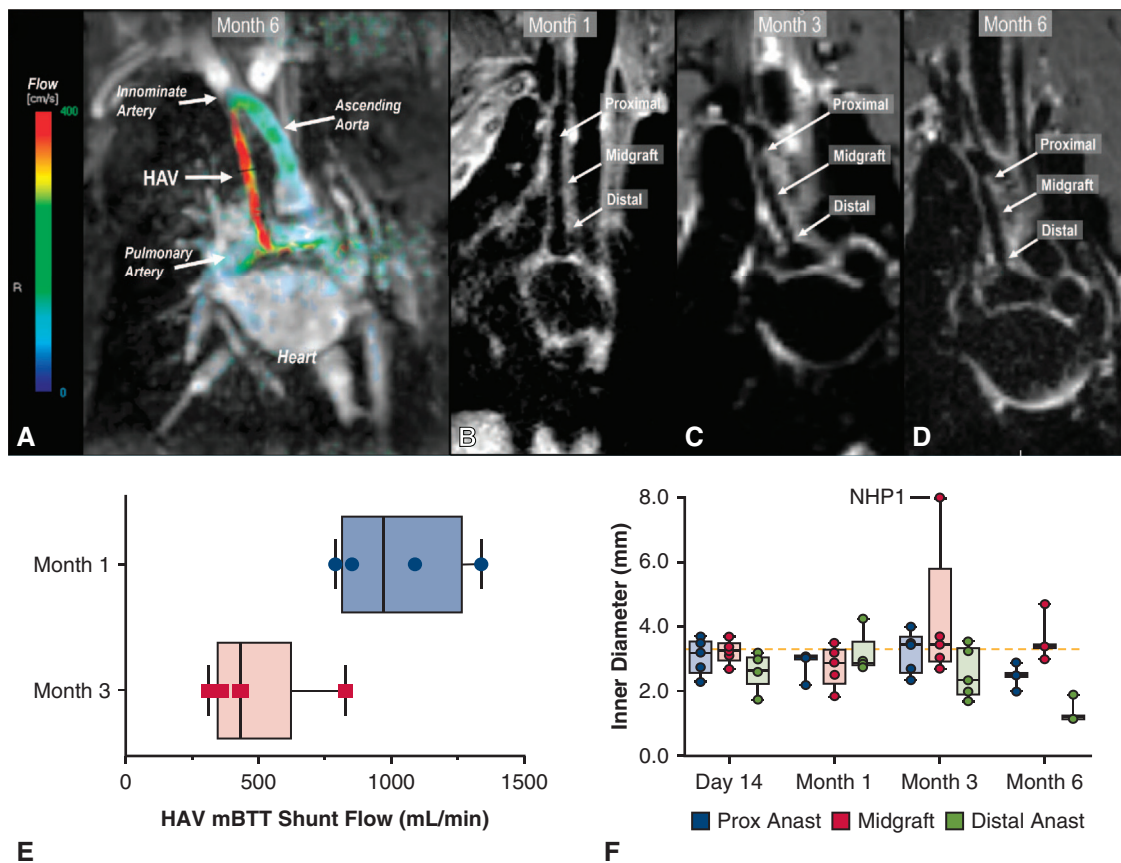
FIGURE 3. Longitudinal MRI and angiographic measurements of HAV mBTT shunts implanted in juvenile NHPs. A, Representative 4-dimensional-flow MRI of blood velocities through the systemic circulation, the HAV mBTT shunt and into the pulmonary artery at 6 months. B-D, Sagittal slices at 1, 3, and 6 months post-implant with inner diameters for proximal, midgraft, and distal regions. E, Peak blood flow velocities within HAV mBTT shunts at months 1 (n = 4) and 3 (n = 5). F, Longitudinal individual measurements for proximal, midgraft, and distal HAV mBTT shunt regions. *Dotted line* indicates size of HAV at implant (3.5 mm). *HAV*, Human Acellular Vessel; *mBTT*, modified Blalock–Taussig–Thomas shunt; *MRI*, magnetic resonance imaging; *NHP*, nonhuman primate.

date. We speculate that the dilatation may have been induced by adaptive immunity with elaboration of proteases, which degraded the structure of the HAV. Interestingly, evaluation of peripheral tissues from NHP1 and NHP3 also revealed evidence of organism-wide adaptive immunity, with reactive lymph nodes and observable immune response in the lung, spleen, and thymus (Figure E3). In contrast, examinations of peripheral tissues from NHP2, NHP4, and NHP5 were unremarkable and did not show signs of systemic immune reaction. Since the only 2 instances of HAV dilatation were seen in animals that also generated a local and peripheral immune response, we hypothesize that the dilatation was caused by host reactivity, as opposed to primary mechanical weakness of the implanted 3.5 mm HAVs.

DISCUSSION

HAVs, engineered from allogeneic smooth muscle cells and then decellularized, have been studied in clinical trials for >9 years. The 6 mm diameter HAV has been evaluated in arteriovenous access for hemodialysis, in the treatment of vascular injury, and in peripheral artery disease. However, a smaller conduit is necessary to address clinical needs in pediatric cardiac and vascular surgery,[29] in adult coronary artery bypass surgery,[30] and in distal revascularization of the limbs.[31] The goal of this study was to evaluate function of a 3.5 mm diameter HAV in a preclinical model of CCHD.

The HAV has shown resistance to infection,[14,15] which is one of the leading causes of mBTTs failure.[32] The HAV is also extensively repopulated and remodeled by host cells,[21] which suggests that the HAV may have the potential to grow along with a growing pediatric patient. The potential for growth of implanted tissue engineered vascular grafts in pediatric patients has been previously shown,[33] and such growth-capable materials could reduce or eliminate the need for repeated operations to revise synthetic conduits in pediatric heart patients.[34,35]

To evaluate the 3.5 mm HAV as a mBTTs conduit, a non-immunosuppressed juvenile NHP surgical model was developed. Healthy animals were implanted with a 2.5- to
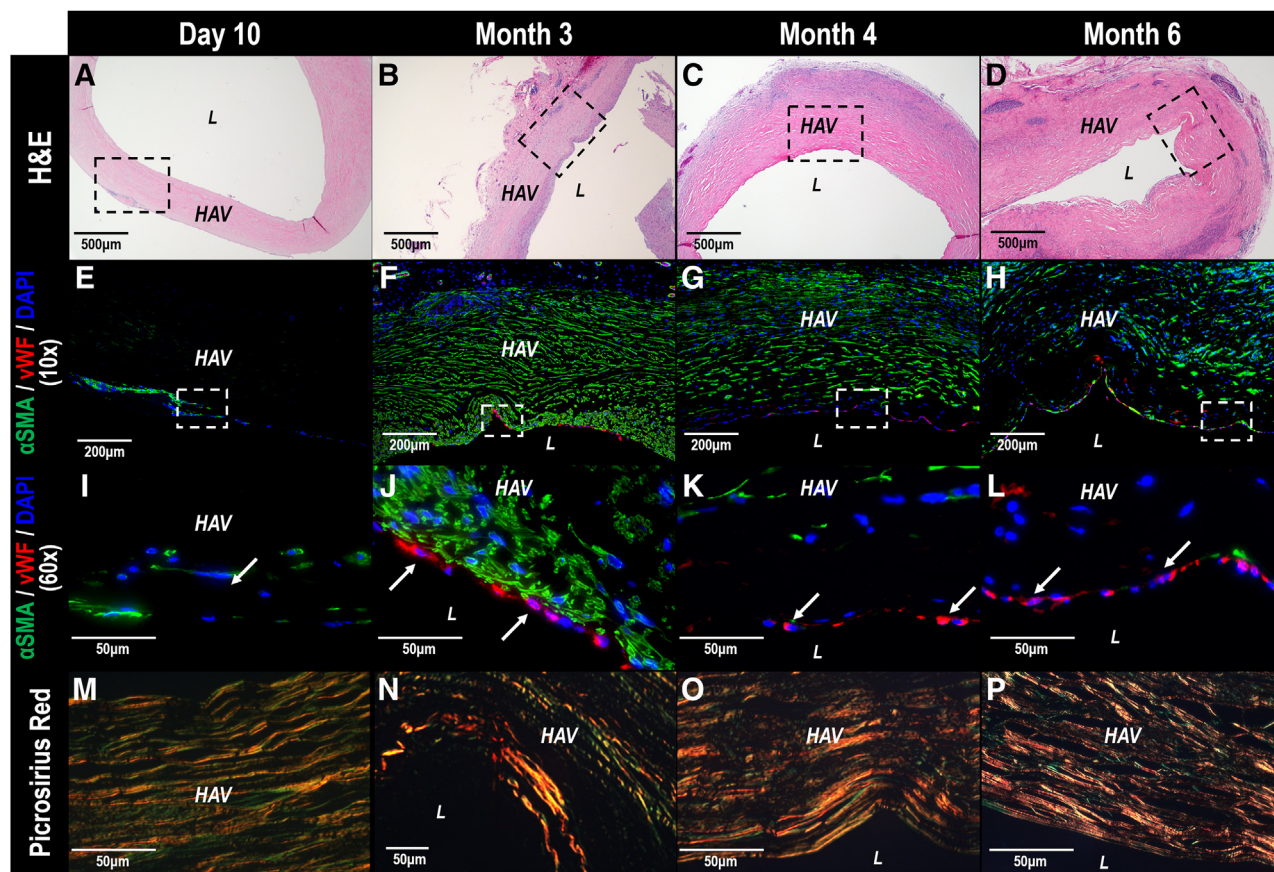
FIGURE 4. Histologic evaluation of host remodeling of HAV mBTT shunts in NHPs over 6 months. HAV explants were stained with H&E (A-D), for *α*-SMA (E-L), vWF (E-L), and with Picrosirius red (M-P) at day 10 (*left column*), month 3, month 4, and month 6. Infiltration of host *α*-SMA$^+$ cells was observed as early as 10 days post-implant, and endothelial cells expressing vWF on the lumen were observed as early as month 3. *H&E*, Hematoxylin and eosin; *HAV*, Human Acellular Vessel; *α-SMA*, smooth muscle actin; *vWF*, von Willebrand factor; *DAPI*, 4′,6-diamidino-2-phenylindole; *mBTT*, modified Blalock–Taussig–Thomas shunt; *NHP*, nonhuman primate.

4.0-cm length of 3.5 mm HAV from the SA to PA and evaluated over 3 to 6 months.[36] Native blood flow through the PA, which would be reduced in infants with CCHD but was not in this healthy animal model, did not appear to compete with flow through the mBTTs. Rather, blood flow persisted through the HAV from the systemic to the pulmonary circulation throughout the experiments. Blood flow rate through the HAV mBTTs, as measured by MRI, was similar to that observed in humans. The blood flow rate decreased from 1 to 3 months, which may have occurred due to narrowing of the HAV as observed in 3- and 6-month explant tissue. A conservative thrombosis prophylaxis approach was taken (postoperative enoxaparin) following intraoperative occlusion of HAV mBTTs in model development NHPs; however, optimization of the distal anastomosis technique in the study animals may have played a larger role in the patency observed.

To date, only 1 previous study of mBTTs in NHPs has been published.[37] In this study, 4-mm diameter ePTFE grafts were implanted as aorta-to-pulmonary mBTTs in 5 animals weighing between 3.6 and 9 kg. Three months after implantation, 2 of the 5 grafts occluded due to thrombosis, resulting in a 40% occlusion rate. The authors also noted that most grafts were narrowed by ~1 mm, primarily at the anastomotic regions with more buildup of tissue at the distal region than the proximal. These data are a useful comparator to the 3.5 mm HAV mBTTs data here and show comparable performance between the conduits despite a significant xenogeneic response to the HAV material in 2 NHPs.

In contrast to the previous reported outcomes with ePTFE in NHPs, all 5 of the implanted HAV mBTTs remained patent for 3 to 6 months. Distal stenosis ≥50% was not observed in any of the HAV mBTTs at 3 months but was identified in 2 of the 3 HAVs at 6 months. This outcome is similar to that observed clinically by Wells and colleagues,[8] wherein 21% of mBTTs were occluded more than 50% at elective take-down. The 3.5 mm HAV therefore seems to perform comparably with historical clinical
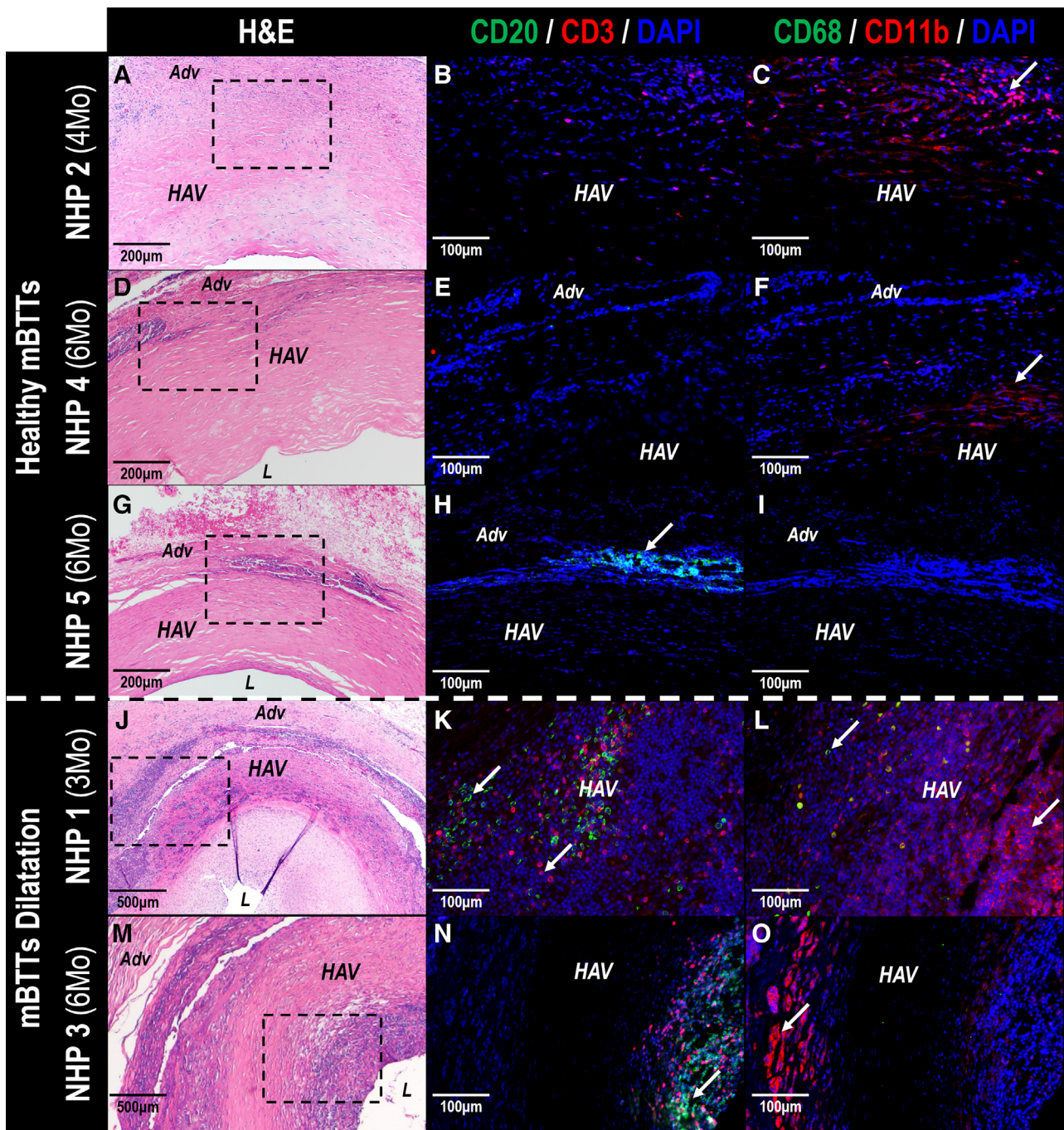
FIGURE 5. Histologic evaluation of host immune response. Midgraft sections from 3.5 mm HAV mBTT shunt explants stained by IHC for CD20 (B-cell), CD3 (T-cell), CD68 (macrophage), and CD11b (monocyte) markers. NHPs with midgraft dilatations (NHP1 and NHP3 [J-O]) exhibited markedly greater levels of host immune infiltration within the mBTT shunt wall than NHPs with no dilatations (NHP2, NHP4, NHP5 [A-I]). Host immune cells in explants from NHP1 and NHP3 were predominantly localized around the regions of dilatation. *H&E*, Hematoxylin and Eosin; *NHP*, nonhuman primate; *HAV*, Human Acellular Vessel; *mBTT*, modified Blalock–Taussig–Thomas shunt; *IHC*, immunohistochemistry; *DAPI*, 4′,6-diamidino-2-phenylindole.

mBTTs data, despite evidence of an intermittent xenogeneic reaction to the HAV human extracellular matrix material in these nonimmunosuppressed animals.

Although rhesus macaques are useful models for xenotransplantation research,[38] implantation of human-derived tissues into rhesus macaques is not well-studied. The HAV is decellularized to remove cellular antigens with the goal of making it non-immunogenic for human implantation. However, chronic implantation in a nonimmunosuppressed, nonhuman model may elicit a xenogeneic response
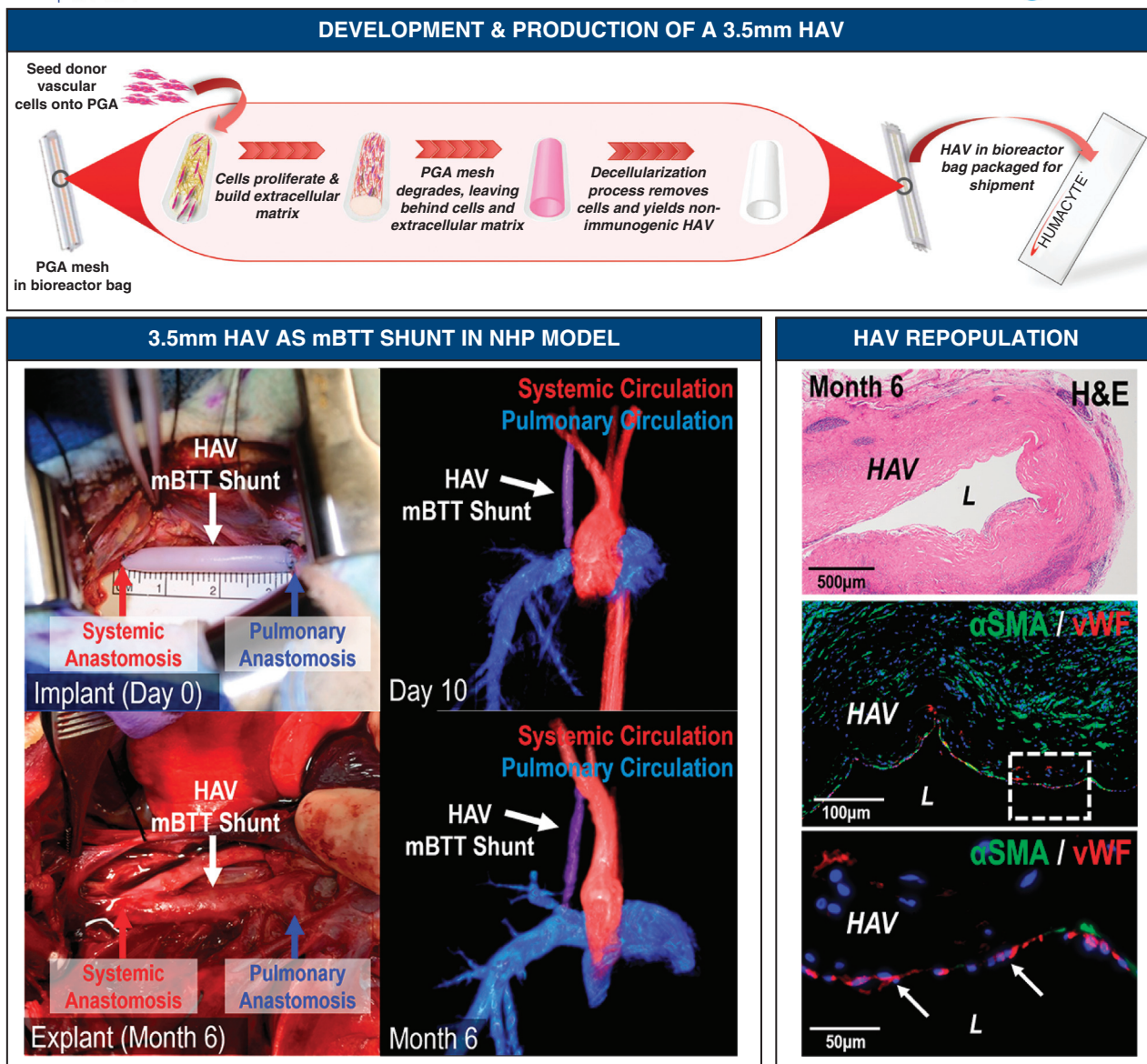
FIGURE 6. The Human Acellular Vessel (HAV; Humacyte, Inc.) production platform was modified to generate 3.5 mm inner diameter HAVs. This small diameter HAV was successfully evaluated for up to 6 months in a nonhuman primate mBTT xenograft model, which demonstrated patency and remodelling with host cells. *PGA*, Polyglycolic acid; *HAV*, Human Acellular Vessel; *mBTT*, modified Blalock–Taussig–Thomas shunt; *NHP*, nonhuman primate; *H&E*, hematoxylin and eosin; *α-SMA*, smooth muscle actin; *vWF*, von Willebrand factor.

to the human extracellular matrix. Since the 6 mm HAV had previously been implanted successfully into baboons for 6 months,[13] we hypothesized that the smaller but phylogenetically related rhesus macaque would tolerate the 3.5 mm HAV as a mBTTs for a similar duration. However, histologic evaluation showed that all mBTTs explants, even those having no dilatation, had regions of T- and B-cell infiltration which were not observed in baboon or human clinical HAV explants to date (Figure 5). Additionally, explants from the

animals with dilated HAVs exhibited systemic evidence of immune reactivity, implying adaptive response to the implanted human matrix. Because the degree of observed systemic immune response was correlated with vessel dilatation, it is likely that the adaptive immune response preceded and precipitated the formation of pseudoaneurysms in NHP1 and NHP3.

Recellularization of mBTTs were observed as early as 10 days postimplant (Figure 4, *A*, model development
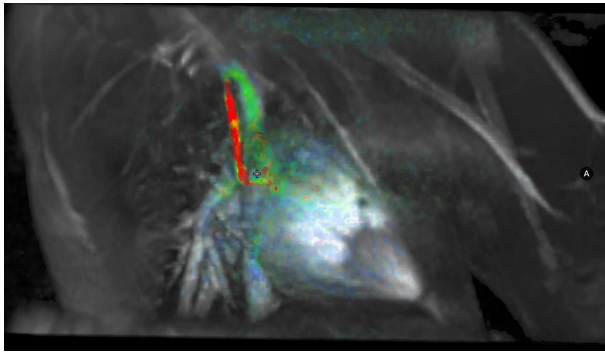
VIDEO 1. Representative MRI 4D flow cine of an HAV mBTTs at 6 months (NHP 4). Video available at: https://www.jtcvs.org/article/S2666-2736(23)00208-5/fulltext.

NHP), with α-SMA$^+$ cells migrating into the HAV primarily from the abluminal surface. Extensive re-population by α-SMA$^+$ cells and partial luminal coverage of vWF$^+$ endothelial cells were noted in explants harvested at 3 to 6 months. This is similar to observations from clinical explants of HAVs, wherein repopulation by α-SMA$^+$ cells by 16 weeks precedes expression of the mature smooth muscle cell marker, calponin 1, and nearly complete endothelial coverage of the HAV lumen by 44 weeks.[21] Thus, recellularization of the HAV in the NHP thoracic cavity seems to mimic what is observed in human implants within more peripheral implantation sites, though further studies are needed to support this finding.

Here, we demonstrated the development of a small-diameter HAV, which was successfully evaluated in an NHP mBTTs surgical model and remained patent in nonimmunosuppressed NHPs for up to 6 months (Figure 6). Since the HAV is repopulated with host cells, an implanted HAV in a juvenile patient may be capable of growing with the patient, potentially reducing or eliminating the need for multiple surgical corrections as the patient ages. However, since these animal recipients had very little somatic growth during these studies, we were not able to assess growth of the HAV here. Further studies are needed to evaluate the HAV's long-term growth potential within juvenile recipients.

Conflict of Interest Statement

The authors employed at Humacyte, Inc, own stock or stock options in Humacyte, Inc. All other authors reported no conflicts of interest.

The *Journal* policy requires editors and reviewers to disclose conflicts of interest and to decline handling or reviewing manuscripts for which they may have a conflict of interest. The editors and reviewers of this article have no conflicts of interest.

References

1. Hoffman JI, Kaplan S, Liberthson RR. Prevalence of congenital heart disease. *Am Heart J*. 2004;147:425-39.
2. Ossa Galvis MM, Bhakta RT, Tarmahomed A, Mendez MD. *Cyanotic Heart Disease*. StatPearls; 2021.
3. Society of Thoracic Surgeons. Society of Thoracic Surgeons Congenital Heart Surgery Data Summary All Patients - Spring 2019 Harvest. Congenital Heart Surgery Database; 2019.
4. Blalock A, Taussig HB. Landmark article May 19, 1945: the surgical treatment of malformations of the heart in which there is pulmonary stenosis or pulmonary atresia. By Alfred Blalock and Helen B. Taussig. *JAMA*. 1984; 251:2123-38.
5. Hines GL. Blalock–Taussig shunt at 75: a landmark operation and a triumph of diversity over prejudice. *Cardiol Rev*. 2019;27:219-21.
6. Klinner W, Pasini M, Schaudig A. Anastomosis between systemic and pulmonary arteries with the aid of plastic prostheses in cyanotic heart diseases. *Thoraxchirurgie*. 1962;10:68-75 [in German].
7. de Leval MR, McKay R, Jones M, Stark J, Macartney FJ. Modified Blalock-Taussig shunt. Use of subclavian artery orifice as flow regulator in prosthetic systemic–pulmonary artery shunts. *J Thorac Cardiovasc Surg*. 1981; 81:112-9.
8. Wells WJ, Yu RJ, Batra AS, Monforte H, Sintek C, Starnes VA. Obstruction in modified Blalock shunts: a quantitative analysis with clinical correlation. *Ann Thorac Surg*. 2005;79:2072-6.
9. O'Connor MJ, Ravishankar C, Ballweg JA, Gillespie MJ, Gaynor JW, Tabbutt S, et al. Early systemic-to-pulmonary artery shunt intervention in neonates with congenital heart disease. *J Thorac Cardiovasc Surg*. 2011;142:106-12.
10. Konig G, McAllister TN, Dusserre N, Garrido SA, Iyican C, Marini A, et al. Mechanical properties of completely autologous human tissue engineered blood vessels compared to human saphenous vein and mammary artery. *Biomaterials*. 2009;30:1542-50.
11. L'Heureux N, Dusserre N, Konig G, Victor B, Keire P, Wight TN, et al. Human tissue-engineered blood vessels for adult arterial revascularization. *Nat Med*. 2006;12:361-5.
12. Canham PB, Finlay HM, Boughner DR. Contrasting structure of the saphenous vein and internal mammary artery used as coronary bypass vessels. *Cardiovasc Res*. 1997;34:557-67.
13. Dahl SL, Kypson AP, Lawson JH, Blum JL, Strader JT, Li Y, et al. Readily available tissue-engineered vascular grafts. *Sci Transl Med*. 2011;3:68ra69.
14. Kirkton RD, Prichard HL, Santiago-Maysonet M, Niklason LE, Lawson JH, Dahl SLM. Susceptibility of ePTFE vascular grafts and bioengineered human acellular vessels to infection. *J Surg Res*. 2018;221:143-51.
15. Wang J, Blalock SKF, Levitan GS, Prichard HL, Niklason LE, Kirkton RD. Biological mechanisms of infection resistance in tissue engineered blood vessels compared to synthetic expanded polytetrafluoroethylene grafts. *JVS Vasc Sci*. 2023;4:100120.
16. Lawson JH, Glickman MH, Ilzecki M, Jakimowicz T, Jaroszynski A, Peden EK, et al. Bioengineered human acellular vessels for dialysis access in patients with end-stage renal disease: two phase 2 single-arm trials. *Lancet*. 2016;387: 2026-34.
17. Dahl SLM, Koh J, Prabhakar V, Niklason LE. Decellularized native and engineered arterial scaffolds for transplantation. *Cell Transplant*. 2003;12:659-66.
18. Dahl SL, Blum JL, Niklason LE. Bioengineered vascular grafts: can we make them off-the-shelf? *Trends Cardiovasc Med*. 2011;21:83-9.
19. ISO7198:2016. Cardiovascular implants and extracorporeal systems — Vascular prostheses — Tubular vascular grafts and vascular patches; 2016:54. Accessed February 18, 2019. https://www.iso.org/standard/50661.html
20. Stacy MR, Best CA, Maxfield MW, Qiu M, Naito Y, Kurobe H, et al. Magnetic resonance imaging of shear stress and wall thickness in tissue-engineered vascular grafts. *Tissue Eng Part C Methods*. 2018;24:465-73.
21. Kirkton RD, Santiago-Maysonet M, Lawson JH, Tente WE, Dahl SLM, Niklason LE, et al. Bioengineered human acellular vessels recellularize and evolve into living blood vessels after human implantation. *Sci Transl Med*. 2019;11:eaau6934.
22. Edelstein AD, Tsuchida MA, Amodaj N, Pinkard H, Vale RD, Stuurman N. Advanced methods of microscope control using muManager software. *J Biol Methods*. 2014;1:e10.

23. Schindelin J, Arganda-Carreras I, Frise E, Kaynig V, Longair M, Pietzsch T, et al. Fiji: an open-source platform for biological-image analysis. *Nat Methods*. 2012; 9:676-82.

24. Ilbawi MN, Grieco J, DeLeon SY, Idriss FS, Muster AJ, Berry TE, et al. Modified Blalock–Taussig shunt in newborn infants. *J Thorac Cardiovasc Surg*. 1984;88:770-5.

25. Tai NR, Salacinski HJ, Edwards A, Hamilton G, Seifalian AM. Compliance properties of conduits used in vascular reconstruction. *Br J Surg*. 2000;87:1516-24.

26. McKenzie ED, Khan MS, Samayoa AX, Vener DS, Ishak YM, Santos AB, et al. The Blalock–Taussig shunt revisited: a contemporary experience. *J Am Coll Surg*. 2013;216:699-704; discussion 704-6.

27. Okita Y, Miki S, Kusuhara K, Ueda Y, Tahata T, Yamanaka K, et al. Acute pulmonary edema after Blalock–Taussig anastomosis. *Ann Thorac Surg*. 1992;53:684-5.

28. Rittie L. Method for picrosirius red-polarization detection of collagen fibers in tissue sections. *Methods Mol Biol*. 2017;1627:395-407.

29. St Peter SD, Ostlie DJ. A review of vascular surgery in the pediatric population. *Pediatr Surg Int*. 2007;23:1-10.

30. O'Connor NJ, Morton JR, Birkmeyer JD, Olmstead EM, O'Connor GT. Effect of coronary artery diameter in patients undergoing coronary bypass surgery. Northern New England Cardiovascular Disease Study Group. *Circulation*. 1996;93:652-5.

31. McPhee JT, Barshes NR, Ozaki CK, Nguyen LL, Belkin M. Optimal conduit choice in the absence of single-segment great saphenous vein for below-knee popliteal bypass. *J Vasc Surg*. 2012;55:1008-14.

32. Sasikumar N, Hermuzi A, Fan CS, Lee KJ, Chaturvedi R, Hickey E, et al. Outcomes of Blalock–Taussig shunts in current era: a single center experience. *Congenit Heart Dis*. 2017;12:808-14.

33. Hibino N, McGillicuddy E, Matsumura G, Ichihara Y, Naito Y, Breuer C, et al. Late-term results of tissue-engineered vascular grafts in humans. *J Thorac Cardiovasc Surg*. 2010;139:431-6, 436.e1-2.

34. Vitanova K, Leopold C, Pabst von Ohain J, Wolf C, Beran E, Lange R, et al. Risk factors for failure of systemic-to-pulmonary artery shunts in biventricular circulation. *Pediatr Cardiol*. 2018;39:1323-9.

35. Dearani JA, Danielson GK, Puga FJ, Schaff HV, Warnes CW, Driscoll DJ, et al. Late follow-up of 1095 patients undergoing operation for complex congenital heart disease utilizing pulmonary ventricle to pulmonary artery conduits. *Ann Thorac Surg*. 2003;75:399-410; discussion 410-1.

36. Apitz C, Webb GD, Redington AN. Tetralogy of fallot. *Lancet*. 2009;374: 1462-71.

37. Braunwald NS, Castaneda AR. Use of the doubly tapered graft for the creation of a systemic-pulmonary arterial shunt. *Ann Thorac Surg*. 1976;22:239-44.

38. Lu T, Yang B, Wang R, Qin C. Xenotransplantation: current status in preclinical research. *Front Immunol*. 2019;10:3060.
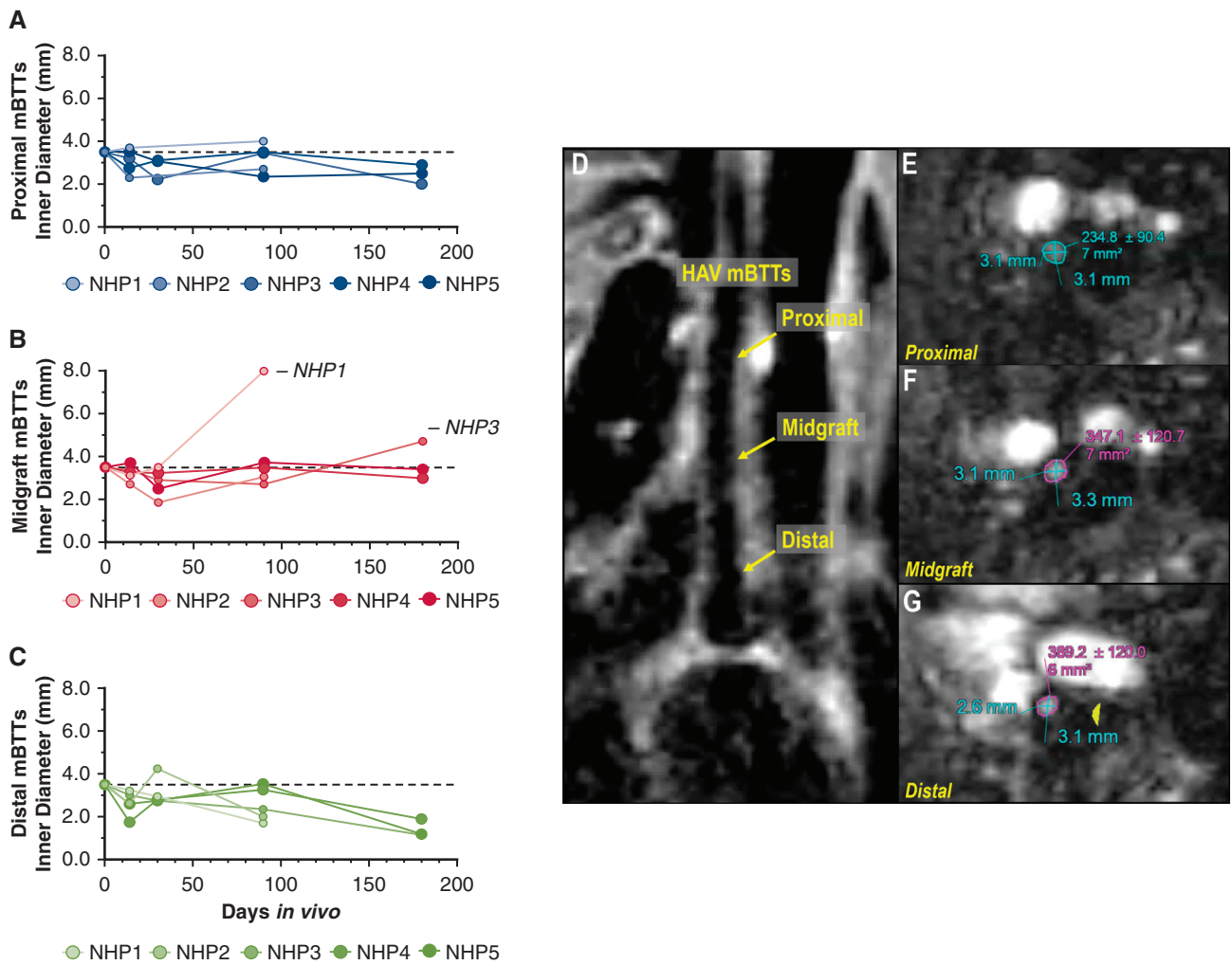
FIGURE E1. Individual NHP longitudinal HAV mBTTs diameter by graft region (A-C). Representative magnetic resonance imaging and cross-sectional mBTTs luminal diameter measurement (D-G). *mBTT*, Modified Blalock–Taussig–Thomas shunt; *NHP*, nonhuman primate; *HAV*, Human Acellular Vessel.
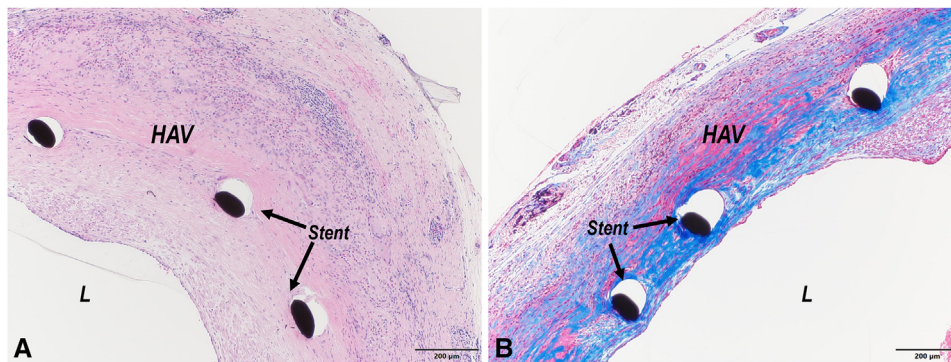
FIGURE E2. Stented HAV mBTTs explant H&E (A) and trichrome (B) histology (NHP 2). *HAV*, Human Acellular Vessel; *mBTT*, modified Blalock–Taussig–Thomas shunt; *H&E*, hematoxylin and eosin; *NHP*, nonhuman primate.
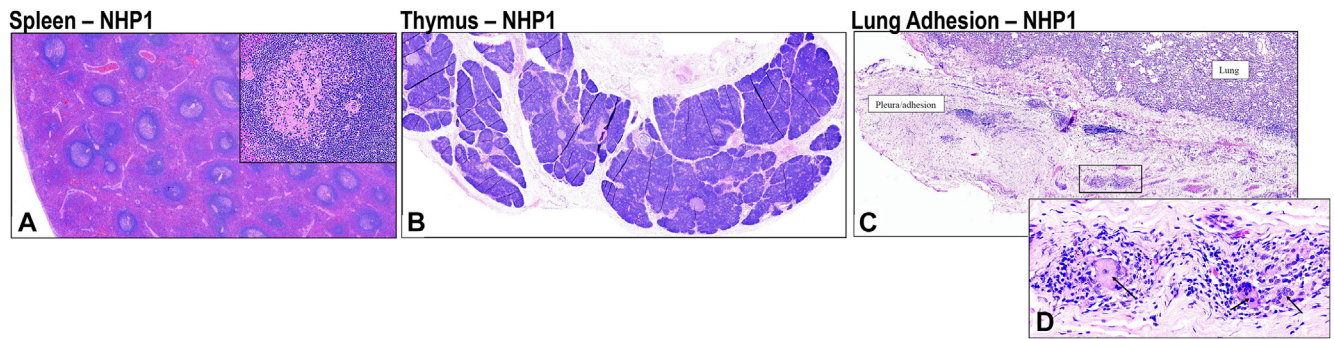
FIGURE E3. A-C, Representative histopathology of immunoreactivity in peripheral tissues of implanted animal with mBTTs midgraft dilatation (NHP 1, 3 months). (D) Lung adhesions displayed mononuclear cell infiltrates that were associated with rare multinucleated giant cells (*black arrow*). *mBTT*, Modified Blalock–Taussig–Thomas shunt; *NHP*, nonhuman primate.